Inhibition of HDAC6 expression decreases brain injury induced by APOE4 and Aβ co-aggregation in rats

YUEXIA DING[1*], AIRONG KANG[2*], QILING TANG[1*] and YING ZHAO[1]

Departments of [1]Pharmacy and [2]Respiration, Yantai Yuhuangding Hospital, Yantai, Shandong 264000, P.R. China

Received March 10, 2019; Accepted July 11, 2019

DOI: 10.3892/mmr.2019.10571

Abstract. The present study aimed to explore the effects of histone deacetylase 6 (HDAC6) on brain injury in rats induced by apolipoprotein E4 (APOE4) and amyloid β protein alloform 1-40 ($A\beta_{1-40}$) copolymerization. The rats were randomly divided into four groups: Control group, sham group, APOE4 + $A\beta_{1-40}$ co-injection group (model group) and HDAC6 inhibitor group (HDAC6 group). The brain injury model was established by co-injection of APOE4 + $A\beta_{1-40}$. Morris water maze experiment was used to observe the spatial memory and learning the ability of rats. Histological changes of the hippocampus were observed by hematoxylin and eosin staining. The mRNA expression levels of choline acetyltransferase (ChAT) and HDAC6 were detected by reverse transcription-quantitative PCR. Immunohistochemistry was used to detect the protein expression of HDAC6. Western blotting was used to detect the protein expression levels of HDAC6, microtubule-associated protein tau and glycogen synthase kinase 3β (GSK3β). APOE4 and $A\beta_{1-40}$ co-aggregation decreased the short-term spatial memory and learning ability of rats, whereas inhibition of HDAC6 activity attenuated the injury. Inhibition of HDAC6 activity resulted in an attenuation of the APOE4 and $A\beta_{1-40}$ co-aggregation-induced increase in the number of dysplastic hippocampal cells. Further experiments demonstrated that APOE4 and $A\beta_{1-40}$ co-aggregation decreased the expression levels of ChAT mRNA, and the phosphorylation levels of tau GSK3β protein in the hippocampus, whereas inhibition of HDAC6 activity resulted in increased expression of ChAT mRNA, tau protein and GSK3β phosphorylation. The inhibition of HDAC6 activity was also demonstrated to reduce brain injury induced by APOE4 and $A\beta_{1-40}$ co-aggregation in model rats.

Correspondence to: Dr Ying Zhao, Department of Pharmacy, Yantai Yuhuangding Hospital, 20 East Yuhuangding Road, Zhifu, Yantai, Shandong 264000, P.R. China
E-mail: yingzhao0964@163.com

*Contributed equally

Key words: histone deacetylase 6, amyloid β protein 1-40, apolipoprotein E4

Introduction

Alzheimer's disease (AD) is the most common type of dementia; it is a degenerative disease of the central nervous system and the main clinical features include progressive memory loss, cognitive impairment and personality changes. According to data released by the International Association of Alzheimer's Disease in 2014, there were ~44,400,000 patients with AD globally, with an annual increase of ~7,700,000 cases, or 1 case every 4 sec (1). The characteristic pathological changes of AD are the formation of the cerebral cortex and senile plaques. The core component of senile plaques is a large amount of fibrous amyloid β protein (Aβ) deposition. Aβ is mainly concentrated in the cerebral cortex and in the hippocampus (2). The neurotoxicity of natural Aβ *in vivo* and *in vitro* has been demonstrated previously (3,4); Aβ plaques may disrupt neuronal excitability, induce axonal varicose veins and neurite rupture, and significantly reduce spinal density (5).

Apolipoprotein E4 (APOE4) is located on chromosome 19 and is a genetic risk factor for AD development (6). Previous studies have reported that APOE4 can induce calcium overload and neuronal death (7), which may lead to multiple spatial memory and work memory damage (8,9) and inhibit hippocampal synaptic plasticity (10). An association has been demonstrated between APOE4 and Aβ plaque loading in the subcortical brain region of patients with mild cognitive impairment. APOE4 enhances the spontaneous fibrogenesis of Aβ peptides and accelerates the aggregation of Aβ *in vitro* (11). Aβ protein metabolism produces a variety of sequence fragments with neurotoxic effects; *in vivo*, $A\beta_{1-40}$ (80-90% of Aβ fragments) and $A\beta_{1-42}$ (10-20% of Aβ fragments) are two types of Aβ protein that are abnormally metabolized by APP, both of which coexist in senile plaques (12).

Histone deacetylase 6 (HDAC6) is a member of the histone deacetylase family, which is comprised of five domains; increased activity of HDAC6 is has been reported to occur in the brain of AD patients (13,14). HDAC6 is a cytoplasmic deacetylase, and previous studies have shown that reduction or inhibition of HDAC6 in AD model mice can improve mouse memory (15). A previous study demonstrated that Aβ-induced mitochondrial axonal transport injury can be rescued by HDAC6 inhibitors in primary neurons (16). Another study

using patient samples indicated that the expression level of HDAC6 was elevated by 52% in the cortex and 91% in the hippocampus, the learning and memory center of the brain, in patients with AD (17,18). Although HDAC6 has great potential as a target for AD therapy (19), the effects of HDAC6 on Aβ and APOE4 co-aggregation on the brain has not been fully understood. In the present study, Aβ and APOE4 co-injection models were established to determine the effects of HDAC6 expression on learning and memory ability and brain injury induced by APOE4 and $A\beta_{1-40}$ co-aggregation.

Materials and methods

Animals and groups. All experiments were conducted in accordance with the Guide for the Care and Use of Laboratory Animals of the National Institutes of Health (20) and have been approved by the Affiliated Yantai Yuhuangding Hospital of Qingdao University Animal Ethics Committee. A total of 36 specific-pathogen-free grade Sprague-Dawley male rats (age, 8-10 weeks; weight, 200±20 g) were purchased from Beijing Weitong Lihua Experimental Animal Technology Co., Ltd. [licence no. SCXK (Jing) 2012-0001]. Rats were provided food and water *ad libitum* and housed in normal laboratory conditions (temperature, 20±2˚C; relative humidity, 40-45%; 12-h light/dark cycle). The rats were divided into the following four groups (n=9/group): i) Control group, which did not receive any treatments; ii) sham group, which received that same surgical procedure (described below) as the model group and were injected with 2 μl sterile saline; iii) Model group, which received surgery and were injected with APOE4 (AMS Biotechnology, Ltd.) + $A\beta_{1-40}$ (Beijing Zhongshan Jinqiao Biotechnology Co., Ltd.); and iv) HDAC6 group, which received surgery and were injected with APOE4 + $A\beta_{1-40}$ as well as HDAC6 inhibitor (10 mg/kg; tubastatin A hydrochloride; cat. no. ab141415; Abcam).

AD model establishment. Rats were anesthetized by intraperitoneal injection of 1% pentobarbital sodium (40 mg/kg) and were fixed on a brain stereotaxic instrument (Rui Wo De). The head and incisors were fixed using the earbuds and the toothed rods. The rats were maintained in the horizontal position, and the surgical area was disinfected with lodophor disinfectant. The skin was separated from the periosteum and blood vessels with a wet cotton swab. A ~2-cm incision was made from the middle of the skull. The CA1 area of the rat bilateral hippocampus was located as previously described (21). A 5-μl microsyringe was fixed on the positioning device holder. Holes were drilled in the skull using the dental drill bilaterally at 3.0 mm posterior to bregma, 2 mm from the skull midline, and the needle was inserted 4.0 mm at each site. The rats in the sham group were injected with 2 μl of sterile saline on each side. The bilateral hippocampus of rats in APOE4 + $A\beta_{1-40}$ group was slowly injected with 1 μl $A\beta_{1-40}$ (10 μg/μl) and 1 μl APOE4 (1 μg/μl) suspension. The needle was kept in the brain for 5 min to ensure adequate dispersion, then the needle was slowly withdrawn. The skull was blocked with dental cement, and the wound was sterilized with sulfamethoxazole (Shanghai Guang Rui Biological Technology Co., Ltd.) to prevent infection and sutured. The animal was kept in a heated chamber until it recovered from anesthesia. At 2 weeks post-surgery, the rats were examined in the Morris water maze experiment.

Morris water maze. For the Morris water maze (130-cm diameter; Anhui Zhenghua Biologic Apparatus Facilities Co., Ltd.) assay, a 15-cm diameter transparent circular platform was placed in the circular pool filled with warm water (25±1˚C) at ~1.5 cm below the water surface. The circular platform was placed in one of the four quadrants in the pool. Rats were trained continuously, with two sessions of four trials each day for 5 days, one in the morning and one in the afternoon. In each session, rats were placed into the water gently, successively in the east, west, south and north quadrants of the maze, with the order remaining consistent for each session. The length of time it took the rats, once placed into the water, to find and climb the platform was recorded as the escape latency. If the rats did not find the platform within 60 sec, they were guided to the platform and allowed to stay on it for 15 sec; after the 15 sec rest period, the next training session was performed, and learning and memory data were recorded.

The platform was removed on day 6, and the rats received four probe trials, in which they were placed into the water in randomly selected quadrants. During these trials, the time to first entry into the previous platform location (T1), time spent in the target quadrant (T2) and number of times that they passed through the previous platform location (N) were recorded; each test lasted for 90 sec. T1, T2 and N for each animal were averaged across the four trials. After the probe tests, the swimming line of rats were examined after placing a visible platform within the pool.

Hematoxylin and eosin (H&E) staining. After the behavioral experiments, brain tissue was removed, and the hippocampus was isolated and fixed in 4% paraformaldehyde (Sangon Biotech Co., Ltd.) at 4˚C overnight. The samples were embedded in paraffin and cut into 4 μm sections. The paraffin sections were dewaxed with xylene, dehydrated with serial dilutions of ethanol, stained with hematoxylin for 10 min at room temperature and eosin for 5 min at room temperature (Beijing Solarbio Science & Technology Co., Ltd.), and rinsed in distilled water for 30 sec. The sections were subsequently washed 2 times (1 min each) with 95% anhydrous and 3 times in xylene (5 min each), and then mounted with Permount mounting medium (Thermo Fisher Scientific, Inc.). Pathological changes were observed under an optical microscope (magnification, x200; Olympus Corporation) and hippocampal neurons cells were counted using Aperio ImageScope v11.1 software (Leica Microsystem GmbH); 5 fields per sample were analyzed for assessment of pathological changes, and the data were expressed as the cell number.

Reverse transcription-quantitative PCR (RT-qPCR). Total RNA was extracted from the hippocampus using a TRIzol kit (Invitrogen; Thermo Fisher Scientific, Inc.). A spectrophotometer was used to determine the purity and integrity of RNA; an optical density (OD)260/OD280 of 1.8-2.0 indicated good RNA purity. cDNA was synthesized by SuperScript III Reverse Transcriptase (Thermo Fisher Scientific, Inc.). cDNA (2 μl) was used for qPCR using a DyNAmo HS SYBR Green qPCR kit (Thermo Fisher Scientific, Inc.). Primers were designed

Table I. Escape latency period of the rats at different time points.

Group (n=9 rats/group)	Day 1 (sec)	Day 2 (sec)	Day 3 (sec)	Day 4 (sec)	Day 5 (sec)
Control	62.93±18.76	34.15±15.35	28.42±13.15	19.52±11.31	14.65±8.01
Sham	64.76±19.54	36.89±16.47	30.56±14.96	21.68±12.52	17.23±9.15
Model	72.76±21.43	63.39±15.97	34.96±15.42	28.86±11.98	26.19±10.23[a]
HDAC6	67.43±20.32	37.26±14.87	32.74±15.13	26.97±11.36	20.86±10.02[a,b]

[a]P<0.05 vs. control. [b]P<0.05 vs. model. HDAC6, histone deacetylase 6.

and synthesized by Shanghai GenePharma Co., Ltd., and the sequences were as follows: HDAC6, forward 5'-TGGCGG ACTAGAAAGAGCCT-3', reverse 5'-GAAGGGGTGACT GGGGATTG-3'; choline acetyltransferase (ChAT), forward 5'-AGCCACTTTCAGTCAGTCGG-3', reverse 5'-ACTCCA GAGTAGCA-3'; β-actin, forward 5'-GTGGGGATAATG AACTTGCAG-3', reverse 5'-GGAACCCCTGGTAGAACA GT-3'. The qPCR thermocycling conditions were: 95˚C for 10 min; followed by 40 cycles at 95˚C for 15 sec and 60˚C for 1 min. β-actin was used as the internal reference and the relative mRNA expression levels were calculated by the $2^{-\Delta\Delta Cq}$ method (22).

Immunohistochemistry. The hippocampal tissues were embedded in paraffin and sectioned (6 μm) (23). The sections were deparaffinized with xylene two times, and rehydrated in a descending ethanol series. Endogenous peroxidase was inhibited by incubating the sections for 30 min with 3% H_2O_2. Antigen retrieval was performed using citrate buffer at high temperature for 10 min. The sections were subsequently blocked for 20 min in 5% BSA, and incubated with anti-HDAC6 primary antibody (1:100; cat. no. ABIN1872957; antibodies-online GmbH) overnight at 4˚C. After rewarming, sections were incubated with a horseradish peroxidase-conjugated goat anti-rabbit IgG secondary antibody (cat. no. ab6721; Abcam) at 37˚C for 1 h; the sections were visualized with 3,3-diaminobenzidine tetrahydrochloride as the chromogen (Beijing Solarbio Science & Technology Co., Ltd.). The sections were subsequently dehydrated and coverslipped with Permount mounting medium (Thermo Fisher Scientific, Inc.). The slides were observed under a x40 optical microscope (Olympus Corporation) and positive-staining cells were counted using Aperio ImageScope v11.1 software (Leica Biosystems Imaging, Inc.); the data were expressed as the percentage of positive cells out of the total number of cells counted.

Western blot assay. Total protein of the hippocampal tissues was extracted using RIPA lysis buffer containing proteinase inhibitor cocktail, and the concentration of protein was determined by bicinchoninic acid assay. Proteins (50 μg) were separated by 10% SDS-PAGE and then transferred onto PVDF membranes (EMD Millipore). The membranes were blocked with 5% skimmed milk at 4˚C overnight, incubated with primary antibodies against HDAC6 (1:1,000; cat. no. ab1440; Abcam); microtubule-associated protein tau (tau; 1:1,000; cat. no. ab64193, Abcam), phosphorylated (p)-tau (phospho-Ser199; 1:1,000; cat. no. ab81268, Abcam); glycogen synthase kinase 3β (GSK3β; 1:1,000; cat. no. 5676; Cell Signaling Technology, Inc.); p-GSK3β (1:1,000; cat. no. 9322; Cell Signaling Technology, Inc.) at 4˚C overnight. After incubating with secondary antibody sheep anti-rabbit IgG (1:5,000; cat. no. ab97095; Abcam) at 37˚C for 1 h, protein bands were visualized using the ECL chemiluminescence system (Thermo Fisher Scientific, Inc.). Protein expression levels were normalized to β-actin (1:2,000; cat. no. ab8227; Abcam) and quantified by Image J software version 1.46 (NIH).

Statistical analysis. SPSS v20.0 statistical software (IBM Corp.) was used for statistical analysis. All the data are expressed as the mean ± SD. Comparisons between two groups was performed using Student's t-test, and multiple groups were compared by one-way ANOVA followed by Fisher's LSD post hoc test. P<0.05 was considered to indicate a statistically significant difference.

Results

HDAC6 inhibition reduces the escape latency of rats. The results of location navigation experiments revealed no significant difference in the escape latency in rats across days 1-4 (Table I). However, the escape latency of the model group (26.19±10.23 sec) and the HDAC6 group (20.86±10.02 sec) were significantly longer compared with that of the control group at day 5 (14.65±8.01 sec; P=0.026 and P=0.034, respectively). There was no significant difference in escape latency on day 5 between the sham group and the control group (P=0.109). The escape latency of HDAC6 group was significantly decreased compared with that of the model group at day 5 (P=0.043).

HDAC6 inhibition reduces the ability of spatial memory of rats. As demonstrated in Fig. 1, the T1 times of the model group and the HDAC6 group rats were significantly increased compared with the control group rats (P=0.019 and P=0.029, respectively; Fig. 1A). The T2 times of the model group and the HDAC6 group rats were also significantly decreased compared with the control group rats (P=0.032 and P=0.047, respectively; Fig. 1B). Compared with the model group, T1 and T2 in the HDAC6 group were significantly different (P=0.033 and P=0.041, respectively). The N of the model and HDAC6 groups was significantly decreased compared with the control group (P=0.021 and P=0.042, respectively; Fig. 1C). N in the HDAC6 group was significantly increased compared

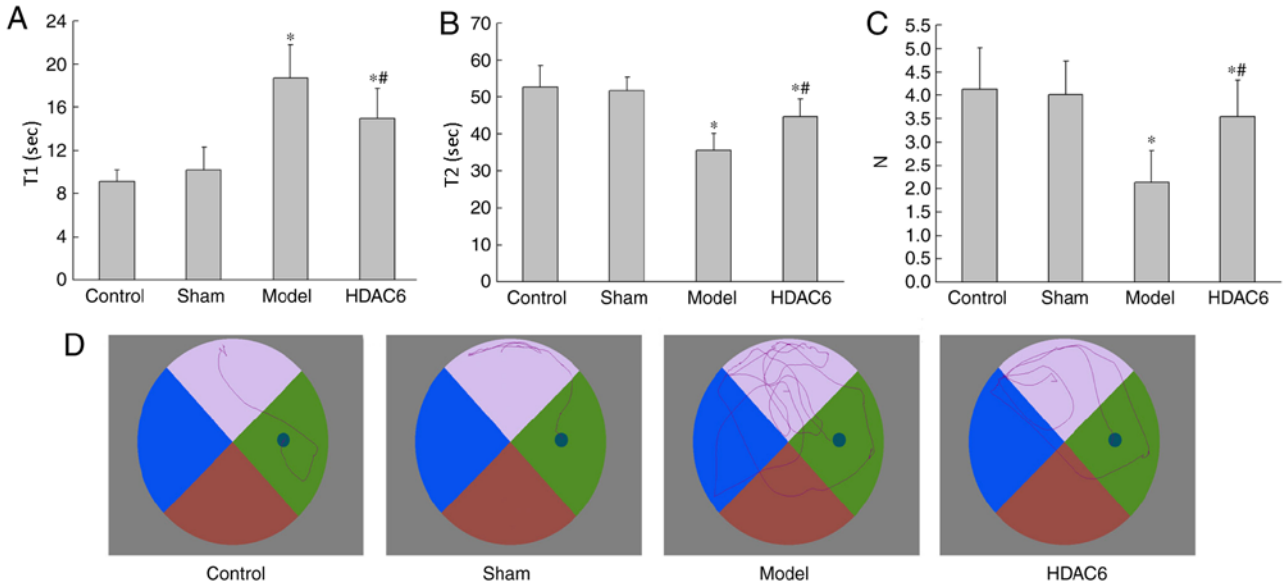

Figure 1. Spatial exploration results in each group. Apolipoprotein E4 (APOE4) and amyloid β protein alloform 1-40 ($A\beta_{1-40}$) co-aggregation increase (A) T1, (B) T2 and (C) N. n=9; *P<0.05 vs. control; #P <0.05 vs. model. (D) Swimming traces on day 6 following the probe test. HDAC6, histone deacetylase 6; N, number of times through the previous platform location; T1, time to first entry into the previous platform location; T2, time spent in target quadrant.

with that in the model group (P=0.036). However. compared with the model group, N was significantly increased for the HDAC6 group (P=0.029; Fig. 1C). In the control and sham group, the rats' swimming line and target were direct; they found the platform in a short time and distance. In the model group, the rats' swimming lines were disordered, meaning they found the platform in a longer time and distance (Fig. 1D). The results showed that APOE4 + $A\beta_{1-40}$ co-injection could decrease the ability of spatial memory of rats, and that inhibition of HDAC6 activity could attenuate the short-term effects on spatial learning ability.

Hippocampal histopathological changes. H&E staining results demonstrated that the control group hippocampus organizational structure was clear and complete, the cells were arranged neatly close, cytoplasm rich, comprising dense surrounding cells without edema (Fig. 2A). Similar morphology was observed in sham group hippocampus (Fig. 2B); the number of hippocampal neurons was not significantly different between the sham group and the control group (Fig. 2E). Hippocampal tissues from model group rats were incomplete, sparse, edematous and irregular, and the number of the neurons were significantly reduced compared with the control group (Fig. 2C and E). The structures of some of the hippocampal neuron cells in the HDAC6 group were partially incomplete, and the number of cells was significantly increased compared with that in the model group (Fig. 2D-E). The results indicated that APOE4 and $A\beta_{1-40}$ co-injection may lead to the development of hippocampal cell dysplasia, and that inhibition of HDAC6 activity may reduce the damage of hippocampal tissues in model rats.

HDAC6 inhibition increases the expression of ChAT mRNA in hippocampus. The effects of APOE4 + $A\beta_{1-40}$ injection on the expression levels of HDAC6 and ChAT mRNA were detected by RT-qPCR. Compared with the control group, the expression of HDAC6 in the model group was significantly increased (P=0.009; Fig. 3A), whereas the expression of ChAT mRNA was significantly decreased (P=0.001; Fig. 3B). Subsequently, in model rats treated with HDAC6 inhibitor, the expression of HDAC6 was significantly decreased (P=0.008) and the expression of ChAT mRNA was significantly increased (P=0.003).

Changes in HDAC6 protein expression. Immunohistochemistry results demonstrated only a few HDAC6-positive cells were observed in the hippocampus in the control group and in the sham group (Fig. 4A and B, respectively). The number of HDAC6-positive cells was higher in the model group (Fig. 4C) as well as in the HDAC6 group (Fig. 4D) compared with the control group, and this increase was significant (Fig. 4E). The percentage of HDAC6-positive cells in the HDAC6 group was significantly lower compared with the model group rats (Fig. 4E); similar result were observed in the western blotting analyses (Fig. 5A and B).

Changes in tau and GSK-3β protein phosphorylation. Compared with the control group, the expression of p-tau protein in the model and in the HDAC6 groups were significantly increased (P=0.0082 and P=0.025, respectively; Fig. 5A and C), whereas the expression of p-GSK-3β protein was significantly decreased (P=0.0042 and P=0.019, respectively; Fig. 5A and D). However, in the HDAC6 inhibitor group, the phosphorylation of tau protein was significantly decreased (P=0.0076; Fig. 5B and D), whereas the phosphorylation of GSK-3β protein was significantly increased (P=0.031; Fig. 5A and D) compared with the model group. The results indicated that inhibition of HDAC6 expression may decrease the damage of APOE4 and $A\beta_{1-40}$ co-aggregation on the brain tissue of rats, and this mechanism may be related to the reduction of p-tau protein content and the increase in GSK-3β protein phosphorylation levels.

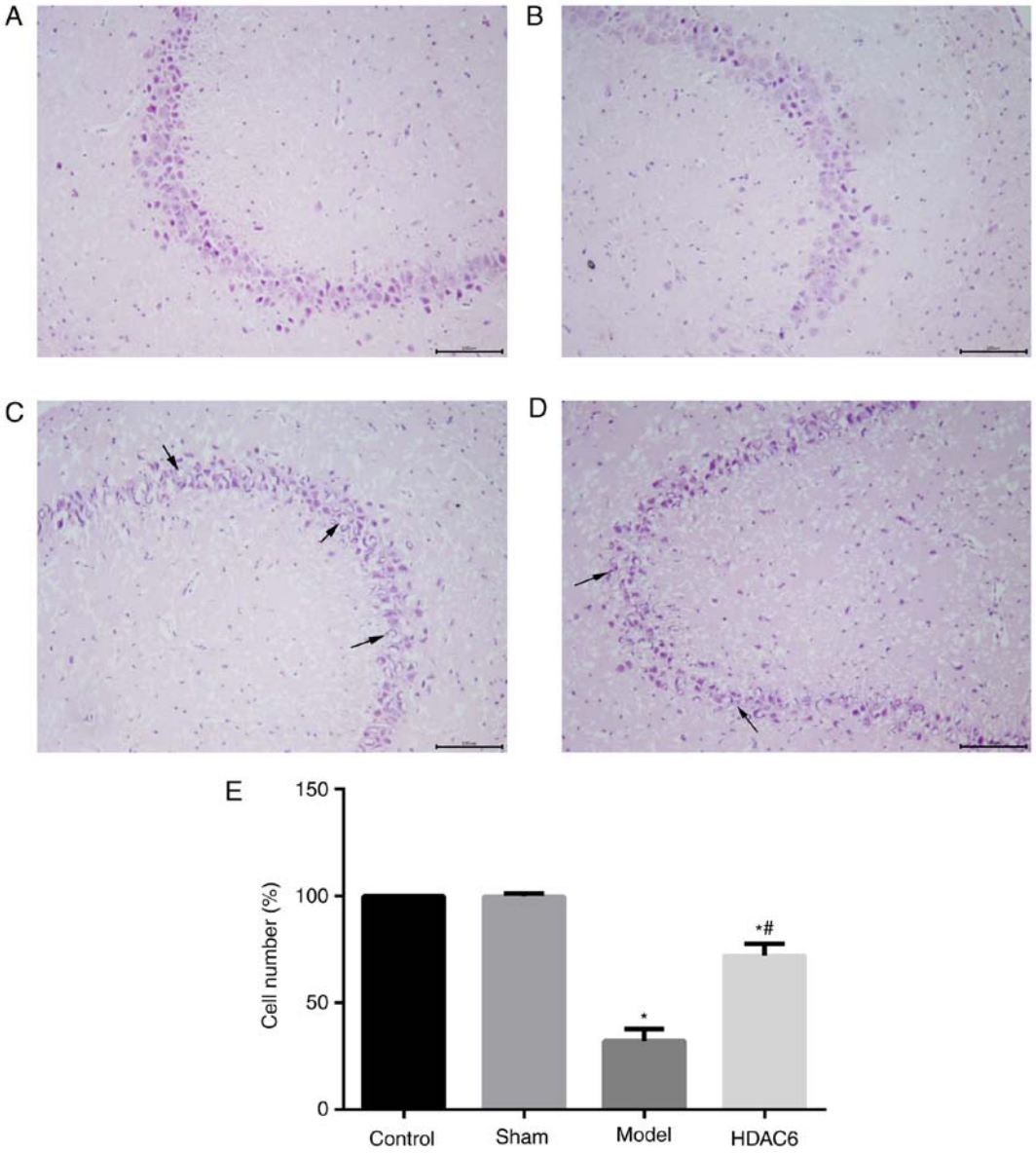

Figure 2. H&E staining of hippocampal tissues. Hippocampal tissues from rats in the (A) control group, (B) sham group, (C) model group and (D) HDAC6 group were stained with H&E. Arrows indicated incomplete hippocampal neuronal cells. Magnification, x200; scale bar, 100 μm. (E) Quantification of hippocampus neuronal cell numbers. *P<0.05 vs. control; $^{\#}$P<0.05 vs. model. H&E, hematoxylin and eosin; HDAC6, histone deacetylase 6.

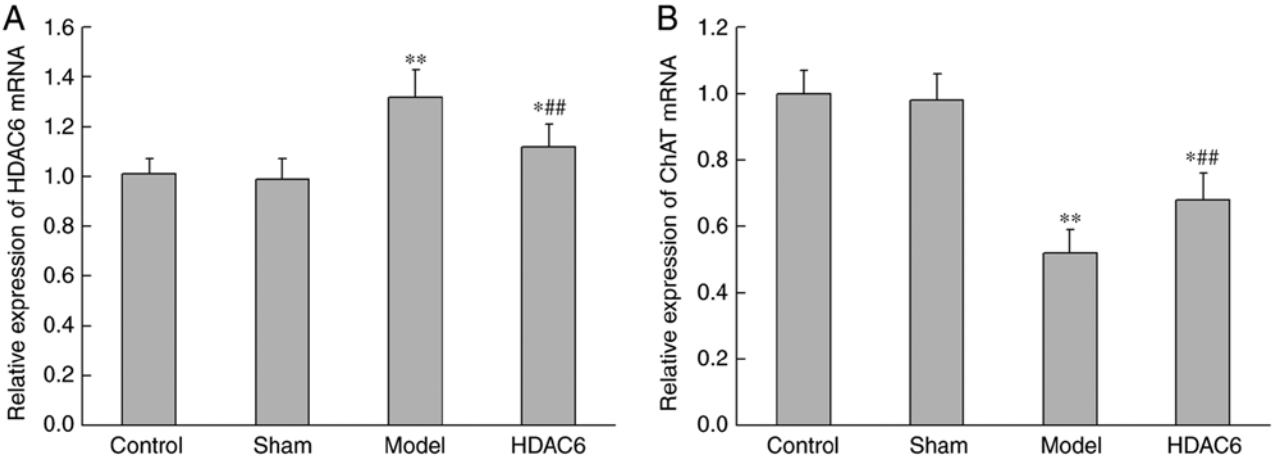

Figure 3. Analysis of HDAC6 and ChAT mRNA expression levels in hippocampus. (A) HDAC6 and (B) ChAT mRNA expression levels were measured by reverse transcription-quantitative PCR. Data are expressed as the mean ± SD. *P<0.05 vs. control; **P<0.01 vs. control; $^{\#\#}$P<0.01 vs. model. ChAT, choline acetyltransferase; HDAC6, histone deacetylase 6.

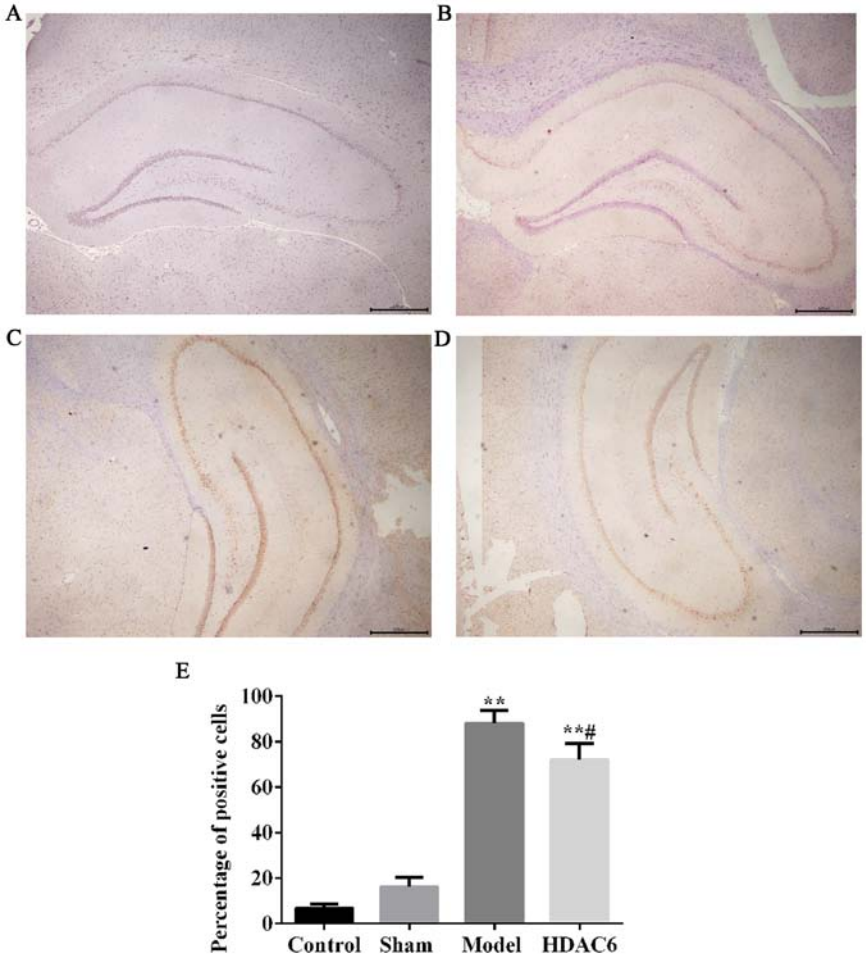

Figure 4. Immunohistochemical analysis of HDAC6 protein expression in hippocampal tissues. Hippocampal tissues from rats in the (A) control, (B) sham, (C) model and (D) HDAC6 groups were stained for HDAC6 expression. Scale bar, 500 μm. (E) Percentage of HDAC6 positive cells from each group. **P<0.01 vs. control; $^{\#}$P<0.05 vs. model. HDAC6, histone deacetylase 6.

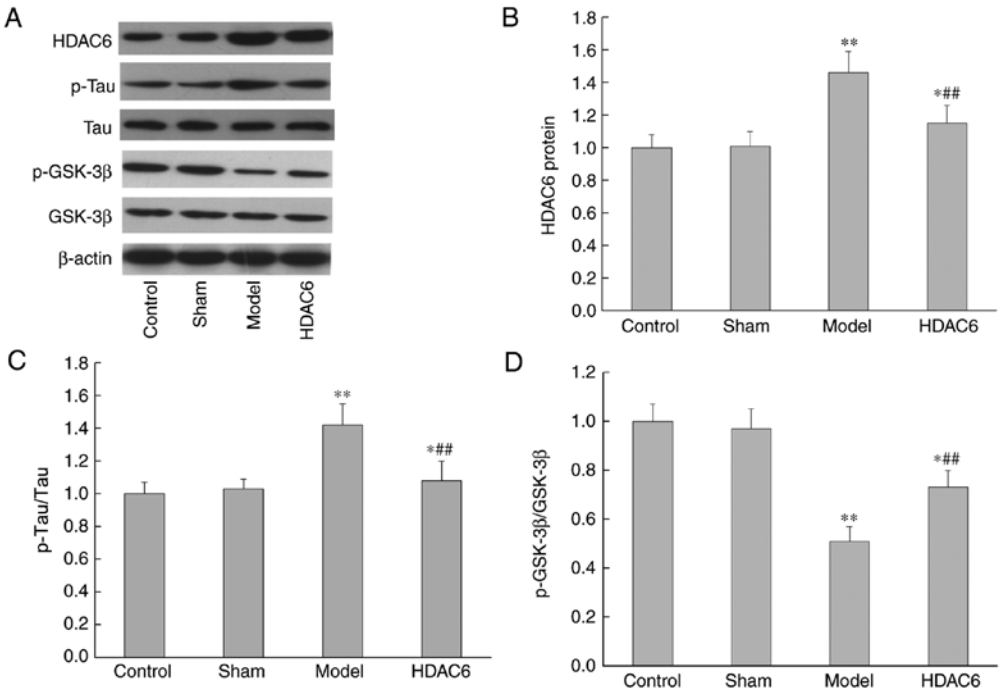

Figure 5. Western blot analysis of HDAC6, p-tau and p-GSK-3β in the hippocampus. (A) Representative western blotting images and (B-D) relative protein expression levels of (B) HDAC6, (C) p-tau and (D) p-GSK-3β. *P<0.05 vs. control; **P<0.01 vs. control; $^{\#\#}$P<0.01 vs. model. GSK3β, glycogen synthase kinase 3β; HDAC6, histone deacetylase 6; p, phosphorylated; tau microtubule-associated protein tau.

Discussion

The etiology and pathogenesis of AD are not yet clear. There are many factors involved, including Aβ deposition, tau hyperphosphorylation, autophagy injury, synaptic transduction, abnormal mitochondria and energy metabolism, abnormal insulin signal transduction pathway, inflammatory injury and oxidative stress (23). Results from the present study indicate that HDAC6 inhibition may have a protective effect on the spatial cognition and learning ability of the model rats, and this mechanism may be related to the hyperphosphorylation of tau protein and dysregulation of the cholinergic system in the hippocampus. The interaction of HDAC6, tau protein and the cholinergic system still needs to be further studied. The effects of Aβ and hyperphosphorylated tau proteins, and their further aggregation and polymerization in AD have received substantial attention in the scientific community. The tau protein is a phosphorus-containing glycoprotein that is encoded by a single gene located on chromosome 17q21, it is a microtubule-associated protein (24). Tau hyperphosphorylation promotes its own integrated oligomers, which can further form neurofibrillary tangles that have significant neurotoxic effects and may affect the formation and stability of microtubules, resulting in axonal transport obstacles (25). The decrease of microtubule stability is an early pathological feature of AD. In addition, tau oligomers may also mediate Aβ toxicity (26). A previous study has reported that HDAC6 and tau proteins affect the stability of microtubules (27). HDAC6 can combine with the tau protein *in vitro* and *in vivo* (28), and promotes the phosphorylation of tau protein (27). The HDAC6 inhibitor can reverse microtubule damage induced by tau hyperphosphorylation (29). HDAC6 inhibitors may reduce the phosphorylation of tau protein by indirect action with GSK3β. In the present study, the expression level of p-tau protein was decreased, and the expression of p-GSK-3β protein was increased following HDAC6 inhibition, which suggested that HDAC6 inhibitors might inhibit the phosphorylation of tau protein by increasing the level of GSK3β to protect the stability of microtubules.

The damage of the cholinergic system in the hippocampus is directly related to the pathogenesis of AD (30). ChAT is a key enzyme in the synthesis of cholinergic neurotransmitters acetylcholine, which is synthesized in cholinergic neurons (31). As such, the expression of ChAT mRNA was investigated to determine the effects of HDAC6 on the damage of cholinergic system in hippocampus. The results demonstrated that the expression of ChAT mRNA was increased following HDAC6 inhibition, which suggested that HDAC6 may affect the function of the cholinergic system by inhibiting the expression of ChAT resulting in AD damage.

In recent years, studies have revealed that HDAC6 expression was increased in the hippocampus and cortex of AD patients (27,32). However, the reasons for this increase and the mechanism are still controversial. Several studies indicated that HDAC6 overexpression may be one of the causes of AD pathogenesis of neurodegenerative disease (27,32,33). It has also been reported that overexpression of HDAC6 may be the result of AD lesions and serve a neuroprotective role in (34,35). Results from the present study were consistent with this. Aβ and APOE4 co-injection models were reported to be better to simulate AD lesions (36). Therefore, the present study established a $A\beta_{1-40}$ and APOE4 co-injection model, which was subsequently treated with an HDAC6 inhibitor, to explore the role of HDAC6 in AD. It was hypothesized that the overexpression of HDAC6 may affect the progression of AD by affecting key enzymes, such as ChAT, in the choline system and microtubule stability. HDAC6 mRNA and protein expression levels were reduced in model rats treated with the HDAC6 inhibitor; it was suggested that the decrease in the expression level of HDAC6 may be caused by the activation of ChAT, tau and GSK3β, and that there may be an interaction feedback loop between them. Whether the specific mechanism is in line with this assumption requires further confirmation studies.

In conclusion, the present study demonstrated that inhibition of HDAC6 expression may improve the cognitive function of rats following $A\beta_{1-40}$ and APOE4 co-aggregation. The results suggested that HDAC6 may be a reliable target for AD therapy.

Acknowledgements

Not applicable.

Funding

No funding was received.

Availability of data and materials

All data generated or analyzed during this study are included in this published article.

Authors' contributions

YD, AK, QT and ZY designed the study; YD, AK, QT and ZY performed the experiments; YD, AK and QT performed data analysis; YD, AK, QT and ZY contributed pathological analysis; YD and AK interpreted the data; YD, AK and QT acquired the samples; YD, AK, QT and YZ wrote the manuscript. All authors read and approved the final manuscript.

Ethics approval and consent to participate

This study was approved by the Ethics Committee of the Affiliated Yantai Yuhuangding Hospital of Qingdao University (Yantai, China).

Patient consent for publication

Not applicable.

Competing interests

The authors declare that they have no competing interests.

References

1. Alzheimer's Disease International. Dementia statistics, 2013.
2. Selkoe DJ and Hardy J: The amyloid hypothesis of Alzheimer's disease at 25 years. EMBO Mol Med 8: 595-608, 2016.
3. Sala Frigerio C and De Strooper B: Alzheimer's disease mechanisms and emerging roads to novel therapeutics. Annu Rev Neurosci 39: 57-79, 2016.

4. Yamin G, Ono K, Inayathullah M and Teplow DB: Amyloid beta-protein assembly as a therapeutic target of Alzheimer's disease. Curr Pharm Des 14: 3231-3246, 2008.
5. Marin MA, Ziburkus J, Jankowsky J and Rasband MN: Amyloid-β plaques disrupt axon initial segments. Exp Neurol 281: 93-98, 2016.
6. Thangavel R, Bhagavan SM, Ramaswamy SB, Surpur S, Govindarajan R, Kempuraj D, Zaheer S, Raikwar S, Ahmed ME, Selvakumar GP, *et al*: Co-expression of glia maturation factor and apolipoprotein E4 in Alzheimer's disease brain. J Alzheimers Dis 61: 553-560, 2018.
7. Qiu Z, Crutcher KA, Hyman BT and Rebeck GW: ApoE isoforms affect neuronal N-methyl-D-aspartate calcium responses and toxicity via receptor-mediated processes. Neuroscience 122: 291-303, 2003.
8. Bour A, Grootendorst J, Vogel E, Kelche C, Dodart JC, Bales K, Moreau PH, Sullivan PM and Mathis C: Middle-aged human apoE4 targeted-replacement mice show retention deficits on a wide range of spatial memory tasks. Behav Brain Res 193: 174-182, 2008.
9. Yin JX, Turner GH, Lin HJ, Coons SW and Shi J: Deficits in spatial learning and memory is associated with hippocampal volume loss in aged apolipoprotein E4 mice. J Alzheimers Dis 27: 89-98, 2011.
10. Chen Y, Durakoglugil MS, Xian X and Herz J: ApoE4 reduces glutamate receptor function and synaptic plasticity by selectively impairing ApoE receptor recycling. Proc Natl Acad Sci USA 107: 12011-12016, 2010.
11. van Bergen JM, Li X, Hua J, Schreiner SJ, Steininger SC, Quevenco FC, Wyss M, Gietl AF, Treyer V, Leh SE, *et al*: Colocalization of cerebral iron with amyloid beta in mild cognitive impairment. Sci Rep 6: 35514, 2016.
12. LaFerla FM, Green KN and Oddo S: Intracellular amyloid-beta in Alzheimer's disease. Nat Rev Neurosci 8: 499-509, 2007.
13. Kuhlmann N, Wroblowski S, Knyphausen P, de Boor S, Brenig J, Zienert AY, Meyer-Teschendorf K, Praefcke GJ, Nolte H, Krüger M, *et al*: Structural and mechanistic insights into the regulation of the fundamental Rho regulator RhoGDIα by lysine acetylation. J Biol Chem 291: 5484-5499, 2016.
14. Fukada M, Hanai A, Nakayama A, Suzuki T, Miyata N, Rodriguiz RM, Wetsel WC, Yao TP and Kawaguchi Y: Loss of deacetylation activity of Hdac6 affects emotional behavior in mice. PLoS One 7: e30924, 2012.
15. Chen S, Owens GC, Makarenkova H and Edelman DB: HDAC6 regulates mitochondrial transport in hippocampal neurons. PLoS One 5: e10848, 2010.
16. Choi H, Kim HJ, Kin J, Kim S, Yang J, Lee W, Park Y, Hyeon SJ, Lee DA, Ryu H, *et al*: Increased acetylation of Peroxiredoxin1 by HDAC6 inhibition leads to recovery of Aβ-induced impaired axonal transport. Mol Neurodegener 12: 23, 2017.
17. Odagiri S, Tanji K, Mori F, Miki Y, Kakita A, Takahashi H and Wakabayashi K: Brain expression level and activity of HDAC6 protein in neurodegenerative dementia. Biochem Biophys Res Commun 430: 394-399, 2013.
18. Zhang L, Sheng S and Qin C: The role of HDAC6 in Alzheimer's disease. J Alzheimers Dis 33: 283-295, 2013.
19. Majid T, Griffin D, Criss Z, Jarpe M and Pautler RG: Pharmocologic treatment with histone deacetylase 6 inhibitor (ACY-738) recovers Alzheimer's disease phenotype in amyloid precursor protein/presenilin 1 (APP/PS1) mice. Alzheimers Dement (N Y) 1: 170-181, 2015.
20. National Research Council (US) Institute for Laboratory Animal Research: Guide for the Care and Use of Laboratory Animals. National Academies Press, Washington, DC, 1996.
21. Paxinos G and Watson C: The Rat Brain in Stereotaxic Coordinates. 6th edition. Hard cover edition, Academic Press, San Diego, CA, 2007.
22. Livak KJ and Schmittgen TD: Analysis of relative gene expression data using real-time quantitative PCR and the 2(-Delta Delta C(T)) method. Methods 25: 402-408, 2001.
23. Jiang S, Nandy P, Wang W, Ma X, Hisa J, Wang C, Wang Z, Niu M, Siedlak S, Torres S, *et al*: Mfn2 ablation causes an oxidative stress response and eventual neuronal death in the hippocampus and cortex. Mol Neurodegener 13: 5, 2018.
24. Stutzmann GE: The pathogenesis of Alzheimers disease is it a lifelong 'calciumopathy'? Neuroscientist 13: 546-559, 2007.
25. Neve RL, Harris P, Kosik KS, Kurnit DM and Donlon TA: Identification of cDNA clones for the human microtubule-associated protein, tau, and chromosomal location of the genes for tau and microtubule-associated protein 2. Mol Brain Res 1: 271-280, 1986.
26. Alonso A, Zaidi T, Novak M, Grundke Iqbal I and Iqbal K: Hyperphosphorylation induces self-assembly of tau into tangles of paired helical filaments/straight filaments. Proc Natl Acad Sci USA 98: 6923-6928, 2001.
27. Lasagna-Reeves CA, Castillo-Carranza DL, Guerrero-Muoz MJ, Jackson GR and Kayed R: Preparation and characterization of neurotoxic tau oligomers. Biochemistry 49: 10039-10041, 2010.
28. Ding H, Dolan PJ and Johnson GV: Histone deacetylase 6 interacts with the microtubule-associated protein tau. J Neurochem 106: 2119-2130, 2008.
29. Noack M, Leyk J and Richter-Landsberg C: HDAC6 inhibition results in tau acetylation and modulates tau phosphorylation and degradation in oligodendrocytes. Glia 62: 535-547, 2014.
30. Xiong Y, Zhao K, Wu J, Xu Z, Jin S and Zhang YQ: HDAC6 mutations rescue human tau-induced microtubule defects in Drosophila. Proc Natl Acad Sci USA 110: 4604-4609, 2013.
31. Orta-Salazar E, Cuellar-Lemus CA, Díaz-Cintra S and Feria-Velasco AI: Cholinergic markers in the cortex and hippocampus of some animal species and their correlation to Alzheimer's disease. Neurologia 29: 497-503, 2014 (In English, Spanish).
32. Li Q, Chen M, Liu H, Yang L and Yang G: Expression of APP, BACE1, AChE and ChAT in an AD model in rats and the effect of donepezil hydrochloride treatment. Mol Med Rep 6: 1450-1454, 2012.
33. Espallergues J, Teegarden SL, Veerakumar A, Boulden J, Challis C, Jochems J, Chan M, Petersen T, Deneris E, Matthias P, *et al*: HDAC6 regulates glucocorticoid receptor signaling in serotonin pathways with critical impact on stress resilience. J Neurosci 32: 4400-4416, 2012.
34. Selenica ML, Benner L, Housley SB, Manchec B, Lee DC, Nash KR, Kalin J, Bergman JA, Kozikowski A, Gordon MN and Morgan D: Histone deacetylase 6 inhibition improves memory and reduces total tau levels in a mouse model of tau deposition. Alzheimers Res Ther 6: 12, 2014.
35. Simões-Pires C, Zwick V, Nurisso A, Schenker E, Carrupt PA and Cuendet M: HDAC6 as a target for neurodegenerative diseases: What makes it different from the other HDACs? Mol Neurodegener 8: 7, 2013.
36. Wu M, He Y, Zhang J, Yang J and Qi J: Co-injection of Aβ1-40 and ApoE4 impaired spatial memory and hippocampal long-term potentiation in rats. Neurosci Lett 648: 47-52, 2017.